Chapter 2

An essential role for UBE2A/HR6A in learning and memory and mGLUR-dependent long-term depression

Caroline F. Bruinsma[1,2], Sanne M. C. Savelberg[1], Martijn J. Kool[1], Mehrnoush Aghadavoud Jolfaei[1], Geeske M. Van Woerden[1,2], Willy M. Baarends[3] and Ype Elgersma[1,2],

[1]Department of Neuroscience, [2]ENCORE Expertise Centre for Neurodevelopmental Disorders, and [3]Department of Developmental Biology, Erasmus MC, Wytemaweg 80, Rotterdam 3015 CN, The Netherlands

Abstract

UBE2A deficiency syndrome (also known as X-linked intellectual disability type Nascimento) is an intellectual disability syndrome characterized by prominent dysmorphic features, impaired speech and often epilepsy. The syndrome is caused by Xq24 deletions encompassing the UBE2A (HR6A) gene or by intragenic UBE2A mutations. UBE2A encodes an E2 ubiquitinconjugating enzyme involved in DNA repair and female fertility. A recent study in Drosophila showed that dUBE2A binds to the E3 ligase Parkin, which is required for mitochondrial function and responsible for juvenile Parkinson's disease. In addition, these studies showed impairments in synaptic transmission in dUBE2A mutant flies. However, a causal role of UBE2A in of cognitive deficits has not yet been established. Here, we show that Ube2a knockout mice have a major deficit in spatial learning tasks, whereas other tested phenotypes, including epilepsy and motor coordination, were normal. Results from electrophysiological measurements in the hippocampus showed no deficits in synaptic transmission nor in the ability to induce long-term synaptic potentiation. However, a small but significant deficit was observed in mGLUR-dependent long-term depression, a pathway previously implied in several other mouse models for neurodevelopmental disorders. Our results indicate a causal role of UBE2A in learning and mGLUR-dependent long-term depression, and further indicate that the Ube2a knockout mouse is a good model to study the molecular mechanisms underlying UBE2A deficiency syndrome.

Introduction

The prevalence of intellectual disability is significantly higher in males compared with females, which is largely due to mutations on the X chromosome (1,2). Of all the males with intellectual disability, ~16% suffer from X-linked intellectual disability (1,2). Recently, the *UBE2A* gene was identified as a cause of X-linked intellectual disability type Nascimento, also known as UBE2A deficiency syndrome, which is caused by mutations in the E2 ubiquitin-conjugating enzyme *UBE2A/HR6A* gene (3). Patients with UBE2A deficiency syndrome are characterized by mild to severe intellectual disability, prominent dysmorphic features, impaired speech, malformations of urinary systems, skin abnormalities and often epilepsy (3–9). Currently, 29 patients with UBE2A deficiency syndrome have been identified, of which 17 patients carried intragenic *UBE2A* gene mutations and 12 patients carried larger deletions encompassing the *UBE2A* gene (3–9).

The UBE2A gene was originally identified as the homolog of *RAD6* (*HR6A*) gene, which plays an important role in DNA damage-induced mutagenesis, mismatch repair and gene silencing (10–12). The *HR6A* gene shares 95% homology with HR6B, which is also a RAD6 homolog. Both genes belong to the family of E2 ubiquitin-conjugating enzymes, which is involved in the ubiquitin proteasome pathway (UPP) required for protein degradation (13). E1 enzymes are responsible for activation of ubiquitin, E2 conjugating enzymes bind the activated ubiquitin and E3 ligases bind the substrates and transfer the conjugated ubiquitin from the E2 enzyme to the substrate. With 600 known members, E3s are the most studied proteins, since they are responsible for substrate recognition. At least 38 E2 genes are known, and only two E1 activating enzymes have been identified (14). Different E2–E3 pairs are known to have very diverse functions (15). Recently, one of the E3 ligases that bind to UBE2A has been identified as Parkin (16). Mutations in Parkin cause juvenile Parkinson, and Parkin has been implied in the ubiquitination of mitochondrial proteins and mitophagy (17,18). Mitophagy deficits were also observed in Drosophila *dRad6* mutants and in cells derived from patients with UBE2A deficiency syndrome. Notably, the *Drosophila dRad6* mutants showed impaired neuronal vesicle trafficking, providing the first causal link between UBE2A and neuronal function (16). Taken together, these studies implied that loss of UBE2A results in mitochondrial dysfunction, which leads to reduced ATP levels, thereby causing the synaptic deficits in *dRad6*mutants.

Previously, a *Ube2a*$^{-/y}$ knockout mouse has been generated to study the role of this gene in reproduction, since research on the paralogue *Ube2b*,showed that *Ube2b* knockout mice have severe spermatogenic deficits (19). Surprisingly, *Ube2a*$^{-/y}$ males showed normal fertility, whereas *Ube2a*$^{-/-}$ females were infertile, suggesting sex-specific roles in reproduction for both homologs (20). However, the presence of neurological deficits in these mice has not been investigated. Here, we used the *Ube2a*$^{-/y}$ knockout mouse to establish a causal link between *Ube2a* mutations and learning disability, and investigated whether these mice suffered from changes in synaptic transmission and synaptic plasticity.

Results

Ube2a$^{-/y}$ mice have no overt motor performance deficit

Patients with the E2 deficiency syndrome display motor delay (3–9). Moreover, UBE2A has been shown to form a functional E2/E3 ubiquitination pair with Parkin, involved in juvenile Parkinson (7). To investigate whether loss of UBE2A causes motor deficits in mice, we made use of *Ube2a*$^{-/y}$ mutants (20). Motor performance was assessed by training the mice on an accelerating rotarod. There was no performance difference between the mutants and wild-type (WT) littermates [$F(1,25) = 0.8$, $P = 0.4$) displayed by a repeated measures ANOVA], and both groups significantly improved their rotarod performance over the 5 days of training (Fig. 1A). To increase the difficulty of the test, we tested the mice on the reverse rotarod at which they have to learn to walk backward. Again, all mice improved in their performance over the 5 days of training, and even though there was a trend toward decreased performance of the mutants, no significant effect of genotype was observed [$F(1,25) = 2.3$, $P = 0.1$ using a repeated measures ANOVA; Fig. 1B].

Hypotonia is also a common feature of UBE2A deficiency syndrome patients (3,5,7,9). To test whether *Ube2a*$^{-/y}$ mutants have reduced muscle strength, we measured their grip strength. No significant differences were observed between the WT mice and the *Ube2a*$^{-/y}$ mice, neither in the front paws [$t(1,25) = 1.4$, $P = 0.2$] nor in all four paws [$t(1,25) = 1.4$, $P = 0.2$] (Fig. 1C).

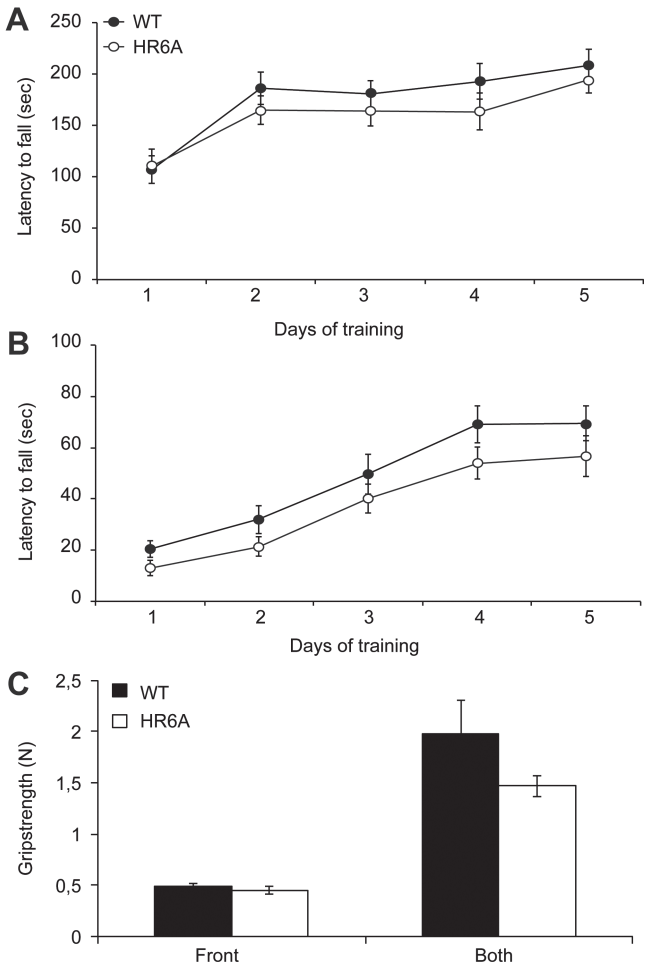

Figure 1: *Ube2a*$^{-/y}$ mice do not show overt motor deficits. (**A**) Rotarod performance of WT mice (black circles) and*Ube2a*$^{-/y}$ mice (white circles) over 5 days. *Y*-axis represents the latency time to fall off the rotating rod. (**B**) Performance on the reversal rotarod also showed no difference in motor performance between WT and *Ube2a*$^{-/y}$ mice. (**C**)*Ube2a*$^{-/y}$ mice (white bars) do not show any muscle strength differences compared with WT mice (black bars) in front paws nor in all four paws (WT $n = 14$ and *Ube2a*$^{-/y}$ $n = 13$ for all experiments shown in A–C). Error bars indicate SEM.

Ube2a$^{-/y}$ mice do not show epilepsy

Approximately half of the E2 deficiency syndrome patients have seizures. There is no clear relation between having an intragenetic mutation or a large deletion, with regard to possibility of developing epilepsy; even patients with the same mutation show difference in prevalence of epilepsy (3–9).

Spontaneous seizures where not observed in *Ube2a*$^{-/y}$ mice; therefore, we tested whether we could induce auditory evoked seizures in these mice, as mouse models for human seizure disorders often have a reduced seizure threshold in this assay (21–23). However, the *Ube2a*$^{-/y}$mice (29 mice tested) showed no induced seizures, indicating that the loss of *Ube2a* is not sufficient for epileptogenesis in mice.

No social behavioral deficits in *Ube2a*$^{-/y}$ mice

Patients with UBE2A deficiency syndrome show behavioral abnormalities (not further specified), which might indicate social dysfunction (3–9). Moreover, autism spectrum disorder is a common comorbidity of syndromes associated with severe intellectual disability such as Fragile X, Rett and tuberous sclerosis complex (TSC) syndrome. Therefore, we tested social behavior in the *Ube2a*$^{-/y}$ mice. Nest building is a natural response behavior displayed by mice for heat preservation, reproduction and shelter and deficient in mouse models of Fragile X, Rett and TSC (23–25). Deficits in nest building were shown to be associated with a variety of brain areas and mainly seen as social dysfunction if the mice are unable to build a nest (26). Both WT mice and *Ube2a*$^{-/y}$ mice displayed a significant increase in nest size $F(6,23) = 71.2$, $P < 0.001$ (Fig. 2A), and no differences between genotypes were observed $F(1,23) = 1.3$, $P = 0.3$. Similarly, *Ube2a*$^{-/y}$ mice also showed no deficits in the Marble burying test, a test that has been used to assess autism-like repetitive movement phenotypes in mice such as Angelman syndrome and Fragile X syndrome (27–31) [$t(1,25) = 0.6$, $P = 0.6$; Fig. 2B]. Taken together, these results indicate that loss of UBE2A does not result in phenotypes commonly seen in mouse models for associated with autism.

Ube2a$^{-/y}$ mice show impaired hippocampal learning

Intellectual disability is a common feature of all patients with UBE2A deficiency syndrome. To investigate if loss of UBE2A is sufficient to induce cognitive deficits in mice, we made use of the Morris water maze task, in which the animal has to learn the location of a hidden escape platform in a pool of opaque water (32). After 7 days of training, WT mice showed a significant reduction in

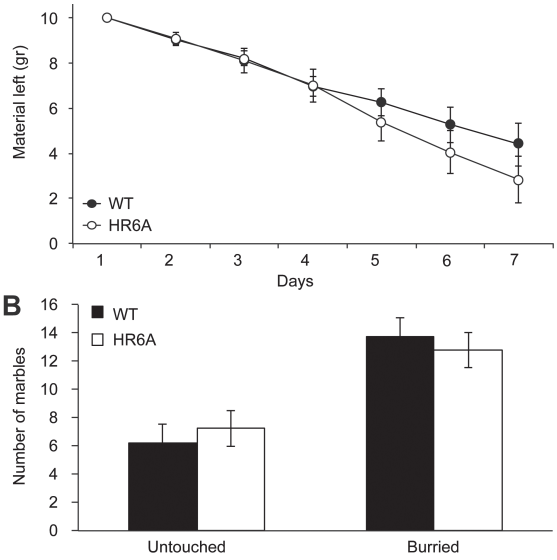

Figure 2: *Ube2a*$^{-/y}$ **mice do not show deficits in nest building and marble burying.** (**A**) Nest-building task showed no difference in the ability to construct a nest between WT mice (black circles) and *Ube2a*$^{-/y}$ mice (white circles) over 7 days, and *Y*-axis represents weight of material left unused (WT $n = 13$ and *Ube2*$^{a-/y}$ mice $n = 12$). (**B**) Testing repetitive, autism-like behavior using the marble burying task showed no increase or decrease in buried marbles between WT mice (black bars) and *Ube2*$^{a-/y}$ mice (white bars) nor in the unburied marbles (WT $n = 14$ and *Ube2a*$^{-/y}$ $n = 13$). Error bars indicate SEM.

escape latency with no significant difference between the two genotypes $F(1,25) = 0.28$, $P = 0.6$ using a repeated measures ANOVA (Fig. 3A). To test whether the mice had learned the spatial location of the platform (hippocampus-dependent spatial learning) or just learned that the platform is at a fixed distance away from the rim (hippocampus-independent procedural learning), we removed the platform at a probe trial given at Day 8 (Fig. 3B). WT mice searched significantly more in the target quadrant when compared with the other quadrants $t(1,25) = 4.3$, $P < 0.05$ (Fig. 3C) and showed significantly more crossings of the platform position compared with similar positions in the other quadrants $t(1,25) = 4.9$, $P < 0.001$ (Fig. 3D), respectively. In contrast, *Ube2a*$^{-/y}$ mutants showed no preference for the target quadrant [$t(1,25) = 0.9$, $P = 0.4$] (Fig. 3C) nor did the mutants show an increased number of platform position crossings (Fig. 3D) compared with other positions [$t(1,25) = 1.2$, $P = 0.2$]. Swim speed in the probe trial was similar between the genotypes [$t(1,25) = 1.1$, $P = 0.3$) suggesting that the deficit was not caused by reduced ability to swim. To control for motivation and inability to perform the water maze test, we performed a visible water maze, in which the

location of the platform is marked. This test demonstrated again no differences between genotypes $F(1,22) = 2.8$, $P = 0.1$ (Fig. 3E). Taken together, these results suggest that the *Ube2a*$^{-/y}$mutants are specifically impaired in the spatial learning component of the water maze test.

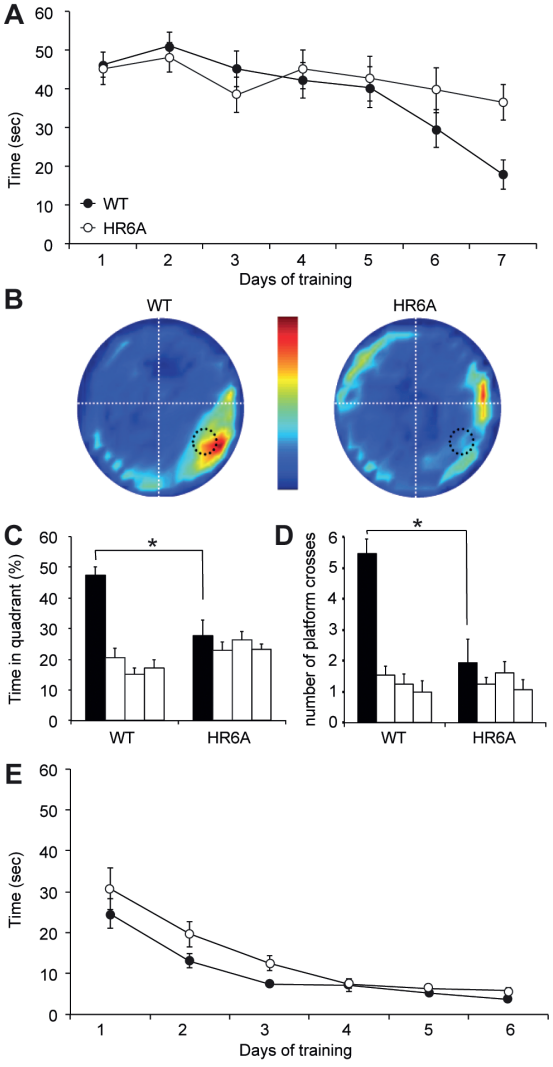

Figure 3: Water maze learning in*Ube2a*$^{-/y}$ mice is impaired. (**A**) Water maze training latencies to reach hidden platform over 7 training days are not different between WT mice (black circles) and*Ube2a*$^{-/y}$ mice (white circles). *Y*-axis indicates average time to reach hidden platform. (**B**) Heat-plot representation of all tracks combined of the probe trial at Day 8. The color represents time spent at a certain location (red is high and blue is low). (**C**) A probe trial at Day 8 shows a clear deficit in *Ube2a*$^{-/y}$ mice with respect to the

time spent searching in the target quadrant (black bar) compared with the average time in the other quadrants (white bar). (**D**) Quantification of the number of platform crosses at each of the four virtual platform positions also shows an impairment in*Ube2a*–/y mice (WT $n = 14$ and *Ube2a*–/y $n = 13$). (**E**) Training latencies in the visible water maze in which the platform is marked and moved every day to a new position. The time to reach visible platform over 6 training days is not different between WT mice (black circles) and *Ube2a*–/y mice (white circles). *Y*-axis represents average time to reach visible platform. Error bars indicate SEM, and asterisks indicate $P < 0.05$.

Hippocampus-dependent learning can also be tested using contextual fear conditioning, in which the animal has to associate a certain context (conditioned stimulus) with an aversive event (foot shock, unconditioned stimulus). There were no differences observed in baseline freezing [$t(1,23) = 0.3$, $P = 0.8$) before the 0.75 mA shock was delivered. However, when context-dependent memory was tested 24 h after training, *Ube2a*$^{-/y}$ mice showed significantly less freezing than WT mice [$t(1,23) = 2.6$, $P < 0.05$). This deficit was still observed when the mice were tested again 7 days after training [$t(1,23) = 3.7$, $P < 0.05$) (Fig. 4A). This fear-conditioning phenotype is not due to decreased sensitivity of the shock, inability to freeze or deficits in amygdala function, because when the shock was paired with a tone as conditioned stimulus, freezing was normal in *Ube2a*$^{-/y}$ mice 24 h after shock [$t(1,23) = 1.0$, $P = 0.3$] and during the long-term memory test [$t(1,23) = 1.3$, $P = 0.20$] (Fig. 4B). Taken together, these results suggest that the *Ube2a*$^{-/y}$ mutants are impaired in learning tests that depend on normal hippocampal function.

No long-term potentiation but a long-term depression deficit in *Ube2a*$^{-/y}$ mice

A previous study showed that loss of the *Drosophila Rad6* gene causes reduced ATP levels due to mitochondrial dysfunction, resulting in impaired vesicle release required for normal synaptic transmission. Given the large body of literature implicating the CA1 Schaffer–collateral pathway in spatial learning, we measured synaptic function and synaptic plasticity of this synapse by making use of extracellular field recordings in acute hippocampal slices. First, we investigated synaptic transmission in *Ube2a*$^{-/y}$ mice. Input–output measures revealed no changes in synaptic transmission, since no differences were observed in the postsynaptic excitatory postsynaptic potentials (fEPSP) slope $F(1,108) = 2.2$, $P = 0.1$ nor in the presynaptic fiber volley amplitude $F(1,108) = 2.3$, $P = 0.6$ (Fig. 5A), nor in the ratio of these

two parameters. This suggests that there are no overt anatomical deficits in *Ube2a*$^{-/y}$ mice. To further investigate if there are changes in presynaptic vesicle release, we measured paired-pulse facilitation (PPF). However, also PPF did not indicate any anomalies in neurotransmitter release as mutant mice were not different from WT mice$F(1,58) = 0.12$, $P = 0.73$ (Fig. 5B).

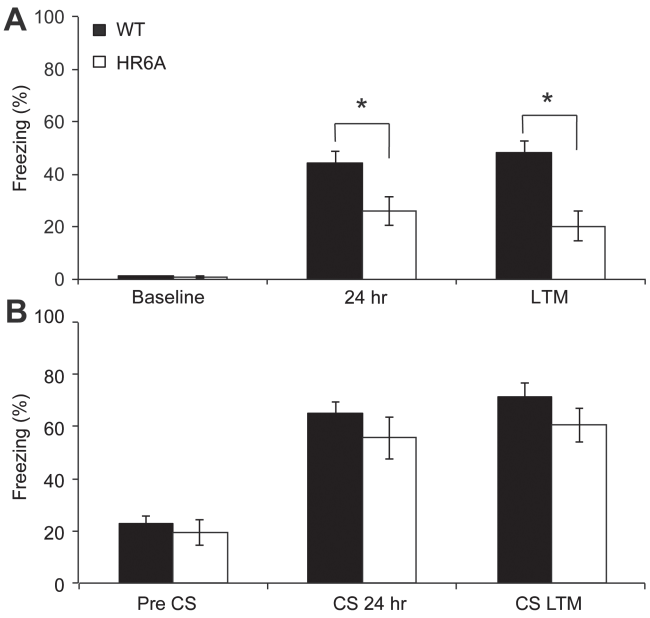

Figure 4: Contextual fear-conditioning deficit in the absence of a cued fear-conditioning deficit in *Ube2a*$^{-/y}$ mice. (**A**) Freezing of the mice is shown at baseline (training before the shock) and during testing 24 h or 7 days [long term memory (LTM)] after the shock. *Ube2a*$^{-/y}$ mice (white bars) show significantly reduced freezing levels compared with WT (black bars). (**B**) Cued (tone) conditioning in which the mice learn to associate the tone (conditioned stimulus; CS) with the shock (unconditioned stimulus) showed no difference in freezing levels between WT and *Ube2a*$^{-/y}$ mice. Pre-CS indicates freezing before onset of the tone, whereas CS 24 h and CS LTM indicate the freezing levels during the tone, 24 h or 7 days after training, respectively. Error bars indicate SEM, and asterisks indicate $P < 0.05$.

Synaptic plasticity, as measured by the ability to induce long-term potentiation (LTP), is thought to be the cellular correlate for learning and memory storage (33). This measure is both sensitive to changes in neurotransmitter release upon high-frequency firing, as well as postsynaptic changes. We measured the ability to induce LTP by using a high-frequency 100 Hz/s stimulus protocol and a more physiological theta-burst stimulation protocol. Despite the profound deficits in spatial learning tasks, we observed

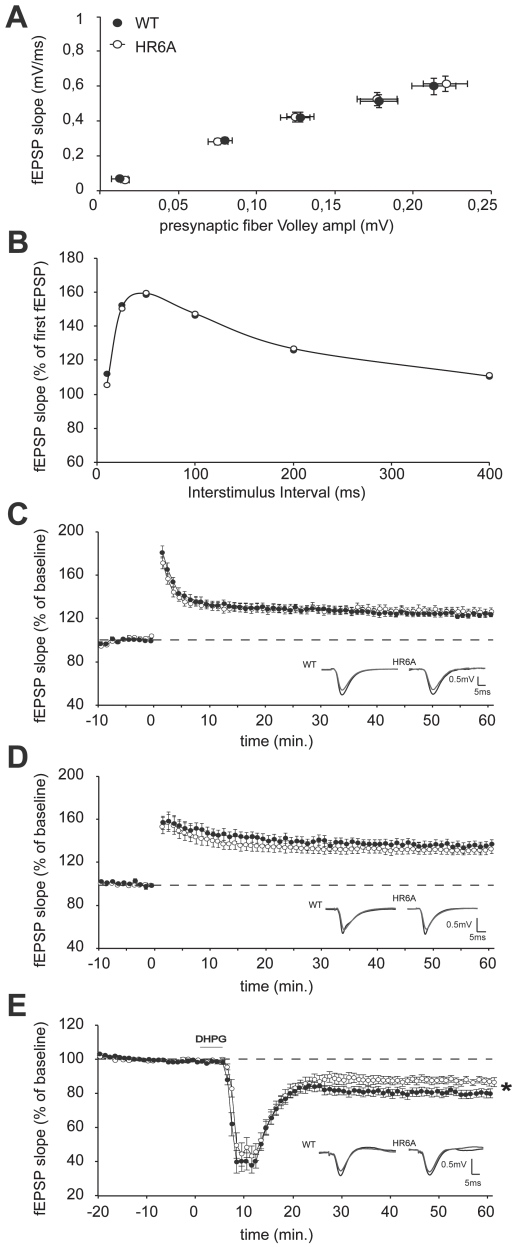

Figure 5: ***Ube2a*$^{-/y}$ mice show reduced mGLUR-dependent LTD at the hippocampal CA3–CA1 synapse.** (**A**) Synaptic transmission (WT *n*= 64, *Ube2a*$^{-/y}$ *n* = 46 slices) and (**B**) PPF (WT *n* = 27, *Ube2a*$^{-/y}$ *n* = 23 slices), a measure of presynaptic function, are unaffected in*Ube2a*$^{-/y}$ mice (white dots). (**C**) LTP induced by a 100 Hz/1 s tetanus (WT *n* = 27, *Ube2a*$^{-/y}$ *n* = 23 slices) or by theta-burst stimulation (WT *n* = 18, *Ube2a*$^{-/y}$ *n* = 18 slices) is not affected in *Ube2a*$^{-/y}$ mice. (**E**) mGLUR5-dependent LTD induced by DHPG application shows a mild but significant deficit in *Ube2a*$^{-/y}$ mice (WT *n* = 33, *Ube2a*$^{-/y}$ = 30). The dashed line shows baseline level before DHPG application. Error bars indicate SEM.

no changes in the ability to induce LTP, as both 100 Hz LTP $F(1.48) = 0.1$, $P = 0.7$ and two-theta LTP $F(1,34) = 0.2$, $P = 0.6$ were unaffected (Fig. 5C and D).
Many studies have shown that impairments in hippocampal long-term depression (LTD) while preserving LTP can also affect learning and memory formation (34,35). A particular form of LTD that depends on the Group I metabotropic glutamate receptors has gained considerable interest, since this form of plasticity is specifically impaired in a mouse model for Fragile X and believed to underlie the cognitive deficits in this mouse model (36–39). Recent studies have also implicated mGLUR signaling impairments in TSC, and convergence of the mTOR and FMRP signaling route (40–44). Moreover, mGLUR LTD deficits were recently observed in a mouse model for Angelman syndrome (45), suggesting that impairments in this pathway may be common to many neurodevelopmental disorders. Hippocampal slices from *Ube2a*$^{-/y}$ mice and their WT littermates were treated with Dihydroxyphenylglycine (DHPG) (50 μM, 5 min), a specific agonist of Group I mGluRs to induce LTD. As shown in Figure 5E, *Ube2a*$^{-/y}$ mice show a moderate but significant reduction in the ability to induce mGluR-dependent LTD $F(1,61) = 5.7$, $P < 0.05$.

Discussion

UBE2A is an intellectual disability syndrome characterized by prominent dysmorphic features, impaired speech and half of the patients display epilepsy. In this study, we tested to what extend mice with mutations in the murine *Ube2a* gene paralleled the disorder and can serve as a model to investigate the underlying pathology.
UBE2A patients show motor delay (3–6), but we found no overt motor deficits in *Ube2a*$^{-/y}$ mice as assessed by rotarod learning and reversal rotarod learning, although it is notable that we consistently found a trend toward mild impairments. Since the patients suffer from motor delay rather than overt motor dysfunction, it could be that our adult mice have overcome such deficits. Hypotonia is a feature seen in around 38% patients (3,5–7,9), but no changes in muscle strength were observed in *Ube2a*$^{-/y}$mice. Since only a quarter of the patients display hypotonia, it is possible that this phenotype is not directly related to the UBE2A mutation or that it requires modifier genes to become apparent.

Likewise, penetrance of the epilepsy phenotype is 50% in the UBE2A patients, but there were neither spontaneous nor evoked audiogenic seizures observed in the *Ube2a*$^{-/y}$ mice. This result suggests that loss of UBE2A is not sufficient to develop epilepsy. Back-crossing the *Ube2a*$^{-/y}$mice in the 129SVE background, which is more permissive to observe seizures (46,47), may potentially reveal an epileptic phenotype.

Consistent with the intellectual disability observed in all UBE2A deficiency syndrome patients described so far, the *Ube2a*$^{-/y}$ mice display clear cognitive deficits as shown in the Morris water maze learning paradigm and the contextual fear-conditioning paradigm. The pronounced deficits in the Morris water maze probe trial, in the absence of a motor deficit or a deficit in the latency to find the platform, indicates the presence of a hippocampal deficit. This was confirmed with the fear-conditioning paradigm where the mice showed a clear context-conditioning deficit, in the absence of a cued-conditioning deficit. Together with, the observation that intellectual disability is observed in all UBE2A deficiency syndrome patients so far implies an essential role of UBE2A in (hippocampus-dependent) learning.

In contrast to the Drosophila studies, we were unable to identify any deficits in presynaptic function, as measured by basal synaptic transmission and PPF. Moreover, mice showed no deficit in LTP induced by high-frequency stimulation, which is very sensitive to changes in neurotransmitter release upon high-frequency firing (48), arguing strongly against an essential role of mammalian UBE2A in vesicle release.

Despite the absence of presynaptic deficits, we found mild changes in hippocampal synaptic plasticity, which is thought to be essential for normal learning. Plasticity deficits (LTP, LTD or both) of the Schafer collateral CA3–CA1 pathway have been reported in most mouse models of intellectual disability disorders like TSC, NF1, Noonan, Rett syndrome, Angelman syndrome and Fragile X (46,49–51). However, the protocol needed to reveal such plasticity deficits varies widely and is likely reflecting the different signaling pathways underlying these plasticity induction protocols. Like the Fragile X mouse model, we found that the plasticity deficit in *Ube2a*$^{-/y}$ mice was specifically observed in the mGluR-dependent induction of LTD. However, unlike Fragile X mice (52), *Ube2a*$^{-/y}$ mice showed impaired LTD rather than enhanced LTD, similar to what has been found in *Tsc1* mutant mice (40–44). Although the ubiquitination and the proteasome have previously been implied in mGluR-

induced LTD, the precise role of this pathway in regulating this form of plasticity remains to be elucidated (45,53–55).

Taken together, our results imply an essential role for UBE2A in hippocampal learning and synaptic plasticity, and provide an attractive mouse model to study the role of UBE2A and the role of protein ubiquitination in learning and memory.

Material and Methods

Subjects

Ube2a$^{-/y}$ male knockout mice (*Ube2a*$^{-/y}$) were generated as described by Roest *et al.* (20). Mice were genotyped at 7–10 days, but the experimenter remained blind for the genotype during data collection and analysis. Genotypes were confirmed after all experiments were finalized, and the code was then broken to perform the final statistical analysis. Mice were housed in groups of 2–4 mice per home cage. Genotype groups were age matched. The mice were kept on a 12 h light/dark cycle, with food and water available *ad libitum*. Behavioral experiments were performed during the light period of the cycle. All animal experiments were approved by the Dutch Ethical Committee and in accordance with Dutch animal care and use laws.

Rotarod

Motor coordination of 3–4 months old mutant and WT littermates was tested on an accelerating Rotarod (model 7650, Ugo Basile, Biological Research Apparatus, Varese, Italy). Mice were measured for 2 trials a day for 5 days with an inter-training interval of 1 h. The Rotarod has a cylinder with a diameter of 3 cm that can accelerate from 4 to 40 rpm in 300 s. The latency to stay on the rotarod was recorded by determining the time taken for a mouse to drop off or stop running for three consecutive rotations. For the reverse rotarod, the same devise was used with added plastic dividers to prevent the mouse from turning around while walking backward.

Marble burying test

Mice were placed in a clean plastic rat cage (Tecniplast 1290D Eurostandard Type 3). The cage contained a 5 cm thick layer of sawdust (Lignocel Hygienic

animal bedding), with 20 dark blue glass marbles (15 mm diameter). The marbles were placed equal distance apart in a grid-like pattern, and the animals were given 30 min to bury them. After 30 min, the number of buried marbles was assed (defined as two-thirds of the marble covered in bedding) by an observer blind to genotype.

Water maze

Prior to start of the water maze, mice were handled for 5 days. The water maze is a circular pool that measures 1.2 m in diameter with a circular platform submerged 1 cm bellow the water (26°C) surface. The light in the room was dimmed, and the water was made opaque using white paint. SMART version 2.0 (Panlab, Barcelona, Spain) was used to track the mice. Mice received 2 trials a day with an inter-trial interval of 30 s. For each trial, the mice were placed on the platform for 30 s and then placed in the pool at pseudorandom positions and allowed to search for the platform for 60 s. If the mouse located the platform, it was allowed to stay on the platform for 30 s before the onset of a new trial. If the mouse was unable to locate the platform, the mouse was placed on the platform by the experimenter for 30 s. This training protocol was repeated for 7 consecutive days. On Day 8, a probe trial was performed. The mouse was placed on the platform, and after 30 s, the platform was removed and the mouse was placed in the water on the opposite side in the bath. The mice were allowed to search for the platform for 60 s.

For the visible water maze test, we used the same paradigm as described for the training sessions in the hidden water maze; the only difference was that the platform was marked and the position of the platform changed with each trial.

Nest building

For measuring nest building, mice were single housed 1 week prior to onset of the experiment. Ten grams of nesting material was provided (thick blot paper biorad170–4085) at the start, and the untouched material was weighed every 24 h for 7 days. This was used to calculate the amount of nest-building material utilized.

Grip strength

Using a force gauge (BIOSEB, Chaville, France) attached to a grid, grip strength was determined by placing the mice with their forepaws and subsequently all

four paws on the grid and steadily pulling the mice by the tail. The grip strength is defined as the maximum strength produced by a mouse before releasing the grid. An average of three trials was taken as an individual performance score for each mouse.

Seizures

To assess seizure susceptibility, we tried to induce an audiogenic seizure by vigorously scraping scissors across the metal grating of a mouse cage lid (creating a high-pitched sound of the 95–105 DB) for 30 s or shorter if a seizure developed before that time.

Fear conditioning

Fear conditioning was performed in a standard modular test chamber located in a standard medium-density fiberboard sound attenuating cubicle (Med Associates, Inc., Albans, VT). The box was equipped with a grid floor on which a 0.75 mA foot shock was delivered. For context conditioning, mice were placed inside the chamber for 180 s after which a foot shock of 2 s was administered after 148 s. After 24 h and after 7 days, the mice were placed back in the chamber and the freezing was measured for 3 min. Freezing was defined as cessation of all movement except for breathing, as quantified using the EthoVision automated video-based algorithm with detection parameters calibrated by independent manual scoring. After context conditioning in Context A, mice were trained again in a Context B, using a 10 kHz tone of 20 s co-terminating with a 2 s foot shock of 0.75 mA. Mice were tested in Context C for cue conditioning 24 h and 7 days later, when the tone was again presented to the mice.

Field recording

Mice were anesthetized and decapitated. Sagittal slices (400 μm) were obtained and submerged in ice-cold artificial cerebrial spinal flued (ACSF) using a vibratome. The hippocampi were subsequently dissected out. The hippocampal slices were left to recover for at least 1.5 h at room temperature before experiments were initiated. After recovery, they were placed in a submerged recording chamber and perfused continuously with ACSF equilibrated with 95% O_2, 5% CO_2 at 31°C at a rate of 2 ml/min. ACSF consisted of (in mM) 120 NaCl, 3.5 KCl, 2.5 $CaCl_2$, 1.3 $MgSO_4$, 1.25 NaH_2PO_4, 26

$NaHCO_3$ and 10 D-glucose. Extracellular recordings of fEPSPs were made in CA1 stratum radiatum with platinum (Pt)/iridium (Ir) electrodes (Frederick Haer Company). A bipolar Pt/Ir was used to stimulate Schaffer collateral/commissural afferents with a stimulus duration of 100 μs. Stimulus–response curves were obtained at the beginning of each experiment 30 min after placing the electrodes. LTP was evoked using the following two different tetani: (1) 100 Hz (1 train of 1 s at 100 Hz) and (2) 4 theta (4 trains of 4 stimuli each at 100 Hz, spaced by 200 ms). The 100 Hz protocol was performed at one-third of the maximum fEPSP and the 4 theta at two-thirds of the maximum fEPSP. LTD was induced after 20 min stable baseline recording with 100 μmol 3,5-DHPG (TOCRIS biosciences) applications for 5 min. LTD was measured at half of maximum fEPSP. During LTP and LTD experiment, slices were stimulated once per minute. Potentiation and de-potentiation were measured as the normalized increase or decrease in the mean fEPSP slope for the duration of the baseline. Only stable recordings were included, and judgment was made blind to genotype. Average LTP and LTD were defined as the mean last 10 min of the normalized fEPSP slope.

Statistical analysis

We used SPSS software for statistical analysis. For rotarod, reversal rotarod, nest building and field recordings, a repeated measures ANOVA with genotype as between-subject factor and time as a within subject factor was used to asses differences. For all other tests, Student's two-tailed *t*-test was used for group comparison on a single variable (e.g. grip strength, time spent in target quadrant, freezing and buried marbles).

Funding

This work was supported by a grant from the Netherlands Organization for Scientific Research (NWO-ZoNMW; VICI grant) to Y.E. and the Erasmus MC fellowship to G.M.V.W.

Acknowledgements

We are grateful to M. Elgersma for technical assistance, and E.J. Mientjes and other members of the Elgersma laboratory for discussion.

Conflict of Interest statement. None declared.

References

1. Ropers, H.H. and Hamel, B.C. (2005) X-linked mental retardation. Nat. Rev. Genet., 6, 46–57.
2. Stevenson, R.E. and Schwartz, C.E. (2009) X-linked intellectual disability: unique vulnerability of the male genome. Dev. Disabil. Res. Rev., 15, 361–368.
3. Nascimento, R.M., Otto, P.A., de Brouwer, A.P. and Vianna- Morgante, A.M. (2006) UBE2A, which encodes a ubiquitinconjugating enzyme, is mutated in a novel X-linked mental retardation syndrome. Am. J. Hum. Genet., 79, 549–555.
4. Budny, B., Badura-Stronka, M., Materna-Kiryluk, A., Tzschach, A., Raynaud, M., Latos-Bielenska, A. and Ropers, H.H. (2010) Novel missense mutations in the ubiquitination-related gene UBE2A cause a recognizable X-linked mental retardation syndrome. Clin. Genet., 77, 541–551.
5. de Leeuw, N., Bulk, S., Green, A., Jaeckle-Santos, L., Baker, L.A., Zinn, A.R., Kleefstra, T., van der Smagt, J.J., Vianne Morgante, A.M., de Vries, B.B. et al. (2010) UBE2A deficiency syndrome: mild to severe intellectual disability accompanied by seizures, absent speech, urogenital, and skin anomalies in male patients. Am. J. Med. Genet. A., 152A, 3084–3090.
6. Honda, S., Orii, K.O., Kobayashi, J., Hayashi, S., Imamura, A., Imoto, I., Nakagawa, E., Goto, Y. and Inazawa, J. (2010) Novel deletion at Xq24 including the UBE2A gene in a patient with X-linked mental retardation. J. Hum. Genet., 55, 244–247.
7. Thunstrom, S., Sodermark, L., Ivarsson, L., Samuelsson, L. and Stefanova, M. (2015) UBE2A deficiency syndrome: a report of two unrelated cases with large Xq24 deletions encompassing UBE2A gene. Am. J. Med. Genet. A., 167A, 204–210.
8. Utine, G.E., Haliloglu, G., Volkan-Salanci, B., Cetinkaya, A., Kiper, P.O., Alanay, Y., Aktas, D., Anlar, B., Topcu, M., Boduroglu, K. et al. (2014) Etiological yield of SNP microarrays in idiopathic intellectual disability. Eur. J. Paediatr. Neurol., 18, 327–337.
9. Czeschik, J.C., Bauer, P., Buiting, K., Dufke, C., Guillen-Navarro, E., Johnson, D.S., Koehler, U., Lopez-Gonzalez, V., Ludecke, H.J., Male, A. et al. (2013) X-linked intellectual disability type Nascimento is a clinically distinct, probably underdiagnosed entity. Orphanet J. Rare Dis., 8, 146.
10. Montelone, B.A., Prakash, S. and Prakash, L. (1981) Recombination and mutagenesis in rad6 mutants of Saccharomyces cerevisiae: evidence for multiple functions of the RAD6 gene. Mol. Gen. Genet., 184, 410–415.
11. Dohmen, R.J., Madura, K., Bartel, B. and Varshavsky, A. (1991) The N-end rule is mediated by the UBC2(RAD6) ubiquitinconjugating enzyme. Proc. Natl. Acad. Sci. USA, 88, 7351–7355.
12. Huang, H., Kahana, A., Gottschling, D.E., Prakash, L. and Liebman, S.W. (1997) The ubiquitin-conjugating enzyme Rad6 (Ubc2) is required for silencing in Saccharomyces cerevisiae. Mol. Cell. Biol., 17, 6693–6699.
13. Ciechanover, A. (2007) Intracellular protein degradation from a vague idea through the lysosome and the ubiquitinproteasome system and on to human diseases and drug targeting: Nobel Lecture, December 8, 2004. Ann. N. Y. Acad. Sci., 1116, 1–28.
14. Deshaies, R.J. and Joazeiro, C.A.P. (2009) RING domain E3 ubiquitin ligases. Annu. Rev. Biochem., 78, 399–434.
15. Glickman, M.H. and Ciechanover, A. (2002) The ubiquitinproteasome proteolytic pathway: destruction for the sake of construction. Physiol. Rev., 82, 373–428.
16. Haddad, D.M., Vilain, S., Vos, M., Esposito, G., Matta, S., Kalscheuer, V.M., Craessaerts, K., Leyssen, M., Nascimento, R.M., Vianna-Morgante, A.M. et al. (2013) Mutations in the intellectual disability gene Ube2a cause neuronal dysfunction and impair parkin-dependent mitophagy. Mol. Cell., 50, 831–843.
17. Chan, D.C. (2006) Mitochondria: dynamic organelles in disease, aging, and development. Cell, 125, 1241–1252.
18. Lee, J.Y., Nagano, Y., Taylor, J.P., Lim, K.L. and Yao, T.P. (2010) Disease-causing mutations in parkin impair mitochondrial ubiquitination, aggregation, and HDAC6-dependent mitophagy. J. Cell Biol., 189, 671–679.

19. Baarends, W.M., Wassenaar, E., Hoogerbrugge, J.W., van Cappellen, G., Roest, H.P., Vreeburg, J., Ooms, M., Hoeijmakers, J.H. and Grootegoed, J.A. (2003) Loss of HR6B ubiquitin-conjugating activity results in damaged synaptonemal complex structure and increased crossing-over frequency during the male meiotic prophase. Mol. Cell Biol., 23, 1151–1162.
20. Roest, H.P., Baarends, W.M., de Wit, J., van Klaveren, J.W., Wassenaar, E., Hoogerbrugge, J.W., van Cappellen, W.A., Hoeijmakers, J.H. and Grootegoed, J.A. (2004) The ubiquitinconjugatingDNA repair enzyme HR6A is amaternal factor essential for early embryonic development in mice. Mol. Cell. Biol., 24, 5485–5495.
21. Puranam, R.S. and McNamara, J.O. (1999) Seizure disorders in mutant mice: relevance to human epilepsies. Curr. Opin. Neurobiol., 9, 281–287.
22. Upton, N. and Stratton, S. (2003) Recent developments from genetic mouse models of seizures. Curr. Opin. Pharmacol., 3, 19–26.
23. Spencer, C.M., Alekseyenko, O., Serysheva, E., Yuva-Paylor, L.A. and Paylor, R. (2005) Altered anxiety-related and social behaviors in the Fmr1 knockout mouse model of fragile X syndrome. Genes Brain Behav., 4, 420–430. Human Molecular Genetics, 2016, Vol. 25, No. 1 | 7 25, 2016
24. Goorden, S.M., van Woerden, G.M., van der Weerd, L., Cheadle, J.P. and Elgersma, Y. (2007) Cognitive deficits in Tsc1+/- mice in the absence of cerebral lesions and seizures. Ann. Neurol., 62, 648–655.
25. Moretti, P., Bouwknecht, J.A., Teague, R., Paylor, R. and Zoghbi, H.Y. (2005) Abnormalities of social interactions and home-cage behavior in a mouse model of Rett syndrome. Hum. Mol. Genet., 14, 205–220.
26. Deacon, R.M. (2006) Assessing nest building in mice. Nat. Protoc., 1, 1117–1119.
27. Deacon, R.M. (2006) Digging and marble burying in mice: simple methods for in vivo identification of biological impacts. Nat. Protoc., 1, 122–124.
28. Huang, H.S., Burns, A.J., Nonneman, R.J., Baker, L.K., Riddick, N.V., Nikolova, V.D., Riday, T.T., Yashiro, K., Philpot, B.D. and Moy, S.S. (2013) Behavioral deficits in an Angelman syndrome model: effects of genetic background and age. Behav. Brain Res., 243, 79–90.
29. Pan, D., Sciascia, A. III, Vorhees, C.V. andWilliams, M.T. (2008) Progression of multiple behavioral deficits with various ages of onset in a murine model of Hurler syndrome. Brain Res., 1188, 241–253.
30. Thomas, A., Burant, A., Bui, N., Graham, D., Yuva-Paylor, L.A. and Paylor, R. (2009) Marble burying reflects a repetitive and perseverative behavior more than novelty-induced anxiety. Psychopharmacology (Berl), 204, 361–373.
31. Zang, J.B., Nosyreva, E.D., Spencer, C.M., Volk, L.J., Musunuru, K., Zhong, R., Stone, E.F., Yuva-Paylor, L.A., Huber, K.M., Paylor, R. et al. (2009) A mouse model of the human Fragile X syndrome I304N mutation. PLoS Genet., 5, e1000758.
32. D'Hooge, R. and De Deyn, P.P. (2001) Applications of the Morriswater maze in the study of learning and memory. Brain Res. Brain Res. Rev., 36, 60–90.
33. Bliss, T.V. (1996) LTP and spatial learning. J. Physiol. Paris, 90, 335.
34. Connor, S.A. and Wang, Y.T. (2015) A place at the table: LTD as a mediator of memory genesis. Neuroscientist., Epub doi: 10.1177/1073858415588498.
35. Mukherjee, S. and Manahan-Vaughan, D. (2013) Role of metabotropic glutamate receptors in persistent forms of hippocampal plasticity and learning. Neuropharmacology, 66, 65–81.
36. Bear, M.F., Huber, K.M. and Warren, S.T. (2004) The mGluR theory of fragile X mental retardation. Trends Neurosci., 27, 370–377.
37. Hou, L., Antion, M.D., Hu, D., Spencer, C.M., Paylor, R. and Klann, E. (2006) Dynamic translational and proteasomal regulation of fragile X mental retardation protein controls mGluR-dependent long-term depression. Neuron, 51, 441– 454.
38. Levenga, J., de Vrij, F.M., Oostra, B.A. andWillemsen, R. (2010) Potential therapeutic interventions for fragile X syndrome. Trends Mol. Med., 16, 516–527.
39. Pop, A.S., Gomez-Mancilla, B., Neri, G.,Willemsen, R. and Gasparini, F. (2014) FragileX syndrome: a preclinical reviewonmetabotropic glutamate receptor 5 (mGluR5) antagonists and drug development. Psychopharmacology (Berl), 231, 1217–1226.

40. Bateup, H.S., Takasaki, K.T., Saulnier, J.L., Denefrio, C.L. and Sabatini, B.L. (2011) Loss of Tsc1 in vivo impairs hippocampal mGluR-LTD and increases excitatory synaptic function. J. Neurosci., 31, 8862–8869.

41. Narayanan, U., Nalavadi, V., Nakamoto, M., Thomas, G., Ceman, S., Bassell, G.J. and Warren, S.T. (2008) S6K1 phosphorylates and regulates fragile X mental retardation protein (FMRP) with the neuronal protein synthesis-dependent mammalian target of rapamycin (mTOR) signaling cascade. J. Biol. Chem., 283, 18478–18482.

42. Auerbach, B.D., Osterweil, E.K. and Bear, M.F. (2011) Mutations causing syndromic autism define an axis of synaptic pathophysiology. Nature, 480, 63–68.

43. Sharma, A., Hoeffer, C.A., Takayasu, Y., Miyawaki, T., McBride, S.M., Klann, E. and Zukin, R.S. (2010) Dysregulation of mTOR signaling in fragile X syndrome. J. Neurosci., 30, 694–702.

44. Chevere-Torres, I., Kaphzan, H., Bhattacharya, A., Kang, A., Maki, J.M., Gambello, M.J., Arbiser, J.L., Santini, E. and Klann, E. (2012) Metabotropic glutamate receptor-dependent long-term depression is impaired due to elevated ERK signaling in the DeltaRG mouse model of tuberous sclerosis complex. Neurobiol. Dis., 45, 1101–1110.

45. Pignatelli, M., Piccinin, S., Molinaro, G., Di Menna, L., Riozzi, B., Cannella, M., Motolese, M., Vetere, G., Catania, M.V., Battaglia, G. et al. (2014) Changes in mGlu5 receptor-dependent synaptic plasticity and coupling to homer proteins in the hippocampus of Ube3A hemizygous mice modeling Angelman syndrome. J. Neurosci., 34, 4558–4566.

46. van Woerden, G.M., Harris, K.D., Hojjati, M.R., Gustin, R.M.,Qiu, S., de Avila Freire, R., Jiang, Y.H., Elgersma, Y. and Weeber, E.J. (2007) Rescue of neurological deficits in a mouse model for Angelman syndrome by reduction of alphaCaMKII inhibitory phosphorylation. Nat. Neurosci., 10, 280–282.

47. Silva-Santos, S., vanWoerden, G.M., Bruinsma, C.F., Mientjes, E., Jolfaei, M.A., Distel, B., Kushner, S.A. and Elgersma, Y. (2015) Ube3a reinstatement identifies distinct developmental windows in a murine Angelman syndrome model. J. Clin. Invest.,125, 2069–2076.

48. Lynch, M.A. (2004) Long-term potentiation and memory. Physiol. Rev., 84, 87–136.

49. Asaka, Y., Jugloff, D.G., Zhang, L., Eubanks, J.H. and Fitzsimonds, R.M. (2006) Hippocampal synaptic plasticity is impaired in the Mecp2-null mouse model of Rett syndrome. Neurobiol. Dis., 21, 217–227.

50. Costa, R.M., Federov, N.B., Kogan, J.H., Murphy, G.G., Stern, J., Ohno, M., Kucherlapati, R., Jacks, T. and Silva, A.J. (2002) Mechanism for the learning deficits in a mouse model of neurofibromatosis type 1. Nature, 415, 526–530.

51. Ehninger, D., Han, S., Shilyansky, C., Zhou, Y., Li, W., Kwiatkowski, D.J., Ramesh, V. and Silva, A.J. (2008) Reversal of learning deficits in a Tsc2+/- mouse model of tuberous sclerosis. Nat. Med., 14, 843–848.

52. Santoro, M.R., Bray, S.M. and Warren, S.T. (2012) Molecular mechanisms of fragile X syndrome: a twenty-year perspective. Annu. Rev. Pathol., 7, 219–245.

53. Citri, A., Soler-Llavina, G., Bhattacharyya, S. and Malenka, R.C. (2009) N-methyl-D-aspartate receptor- and metabotropic glutamate receptor-dependent long-term depression are differentially regulated by the ubiquitin-proteasome system. Eur. J. Neurosci., 30, 1443–1450.

54. Colledge, M., Snyder, E.M., Crozier, R.A., Soderling, J.A., Jin, Y., Langeberg, L.K., Lu, H., Bear, M.F. and Scott, J.D. (2003) Ubiquitination regulates PSD-95 degradation and AMPA receptor surface expression. Neuron, 40, 595–607.

55. Hegde, A.N. (2010) The ubiquitin-proteasome pathway and synaptic plasticity. Learn. Mem., 17, 314–327.